Antiplasticization and the elastic properties of glass-forming polymer liquids

Robert A. Riggleman,[a] Jack F. Douglas[b] and Juan J. de Pablo*[c]

Received 30th July 2009, Accepted 28th October 2009
First published as an Advance Article on the web 24th November 2009
DOI: 10.1039/b915592a

We investigate the effect of antiplasticizer additives on long-wavelength thermodynamic properties relating to the efficiency of molecular packing (density ρ and isothermal compressibility κ_T) and material stiffness (bulk modulus K, shear modulus G, and Poisson ratio ν) of model glass-forming polymer melts. Variations in the stiffness (G and molecular force constant k_m from the Debye–Waller factor $\langle u^2 \rangle$) and density ρ at a molecular scale are also considered. We find that antiplasticizer additives cause significant changes in the long-wavelength properties that are associated with an enhanced packing efficiency in the glass state, such as a decrease in κ_T and an increase in K, G, and ν. Moreover, values of the local elastic moduli in the glass state follow a nearly universal (approximately log-normal) distribution and a Fourier transform of the elastic constant fluctuations in space reveals a general -2 wave vector q scaling, as in order parameter fluctuations in critical fluids and magnetic systems near their critical point for phase separation and ordering, respectively. No discernible large-scale fluctuations in the density were observed, however, indicating that the local elastic constant fluctuations do not reflect density (free volume) fluctuations, as often assumed. These observations provide essential insights into how varying the fragility of glass formation, through the addition of antiplasticizer additives, alters the local mechanical properties of polymer melts and other glass-forming liquids.

I. Introduction

The addition of antiplasticizer additives to polymeric and other glass-forming liquids can have a dramatic influence on the thermophysical properties of these materials. Antiplasticizers influence material stiffness, brittleness and gas permeability in the glass state, as well as properties related to processibility (*e.g.*, viscosity, stress relaxation time, diffusion coefficient) of the polymer melt. Applications are manifold, but recently there has been particular interest in these additives as a means of stabilizing polymer nanostructures against mechanical failure and as a preservation matrix for protein-based drugs and other biological materials.[1,2]

In previous work,[3–5] we have introduced coarse-grained simulation models of polymeric systems that capture the basic property changes that serve to define the antiplasticization phenomenon in real materials. In particular, antiplasticizer additives increase both the density and the shear modulus in the glass state relative to the pure polymer melt,[6,7] while simultaneously decreasing the (primary or α) structural relaxation time and glass transition temperature, T_g. We show below that these changes are associated with changes in packing efficiency[8–12] (or packing frustration) that engender a change in the very nature of glass formation rather than just a change in T_g.[12] Specifically, the antiplasticizer enhances packing efficiency (*i.e.*, density ρ) in the glass state and renders the polymer melt a stronger glass-forming liquid.[3–5,13] A variety of measures of fragility (a measure of the strength of the temperature dependence of the structural relaxation time relative to the Arrhenius relation, more fragile fluids exhibiting a relatively strong temperature dependence) were considered to establish this interpretation of the effect of antiplasticization in terms of changes in the fragility of glass formation. We also confirmed that the reduction in fragility of glass formation by the antiplasticizer had the effect of reducing the relative scale of collective (specifically, string-like) particle motion,[3,4] as required by the identification of these structures with the cooperatively rearranging regions of the Adam–Gibbs structural relaxation model.[14]

The present work focuses on the phenomenon of antiplasticization from a different perspective. Our ability to tune the fragility of glass formation with antiplasticizer additives leads to questions of how the elastic properties of these polymer melts become modified as the fragility of glass formation is varied, a phenomenon of evident importance to understanding the nonlinear deformation properties of polymeric materials and for further understanding the physical origin of fragility variations in glass-forming liquids. The entropy theory of glass formation of Dudowicz *et al.*[12] indicates a general interpretation of fragility variations in glass-forming liquids in terms of variable molecular packing efficiently or 'packing frustration' and, given the broad accord that has been observed between simulations and this theory in previous work,[3,4] we may expect variations in the local packing efficiency to reflect themselves in the mobility, compressibility, and elastic constants of the material. This would seem to offer an obvious origin of the often observed

[a]*Department of Chemical Engineering, University of California-Santa Barbara, Santa Barbara, CA, 93106, USA*
[b]*Polymers Division, National Institute of Standards and Technology, Gaithersburg, Maryland, 20899, USA*
[c]*Department of Chemical and Biological Engineering, University of Wisconsin-Madison, Madison, Wisconsin, 53706, USA. E-mail: depablo@engr.wisc.edu*

dynamically heterogeneous nature of glass-forming liquids[14–21] and should make an investigation of the elastic properties particularly interesting. In particular, there is the question of how dynamical heterogeneity, defined in terms of particle mobility, is related to heterogeneity in the elastic constants of the medium. We also expect non-trivial changes in the Poisson ratio associated with packing frustration, as found in granular materials[22] and other complex 'jammed' materials.

Our investigation first considers long-wavelength properties related to stiffness and the antiplasticization phenomenon such as the density, isothermal compressibility, bulk modulus, shear modulus and the Poisson ratio. These properties are considered over a wide range of temperatures for both a fragile pure polymer melt and a relatively strong antiplasticized polymer melt investigated in previous work. We find an intriguing tendency for many of these properties to cross as the temperature is varied so that a variation of fragility (or antiplasticizing additive) can have opposing effects on these basic properties, depending on temperature. This observation, which is commonly observed in the density and shear modulus of real antiplasticized materials,[23,24] seems to be particularly relevant to the Poisson ratio ν, where a variation of fragility of glass formation has an opposite effect on the Poisson ratio at temperatures above and below T_g. Clearly, this is an important issue in relation to recent attempts to correlate the fragility of glass-forming liquids to the Poisson ratio[25] and the observation of contrary trends in this relationship.[26]

We next turn to characterizing the local elastic properties of the pure and antiplasticized polymer materials. To do this, we calculate the local elastic constants within these samples by measuring the local stress and strains that develop following a macroscopic deformation.[27] Averaging these local elastic moduli recovers the long-wavelength elastic modulus, but more generally we obtain a 'map' of the local stiffness of the material, which can range from locally very stiff (large modulus) in some regions to 'soft' regions where the apparent modulus is formally negative[27] as a consequence of the packing frustration within the material. We find that the nature of these elastic constant fluctuations depends quite strongly on the fragility of the glass-forming liquid. We also consider the Debye–Waller factor, $\langle u^2 \rangle$, which represents the mean-square particle displacement (averaged over all particles after a time in the caging regime[28] where the particles are transiently localized), which provides another local measure of the 'stiffness' in the material at an atomic scale.[29] Specifically, $k_BT/\langle u^2 \rangle$, where k_BT is the thermal energy, can be taken as a measure of the local force constant k_m and we might expect local relative variations in k_m to be comparable, at least qualitatively, with the local elastic modulus. We indeed find that these properties track each other to some degree, supporting the heuristic interpretation of k_m as a 'local elastic constant'.[29] The practical value of this correspondence is that the computation of k_m can readily be extended to temperatures much higher than T_g, while the elastic constant calculations require the temperature to be near or below T_g. It is thus possible to explore the local elastic properties of glass-forming liquids at higher temperatures to gain further insight into the relation between stiffness fluctuations and the dynamic heterogeneity phenomenon of glass-forming liquids. Previous work by Harrowell and Widmer-Cooper,[30] and subsequently by us,[3] has shown that particle mobility in the supercooled liquid regime above T_g correlates rather well with $\langle u^2 \rangle$, based on the same method of computing $\langle u^2 \rangle$ employed as in the present paper. The distributions of the shear elastic constant are found to generally follow an asymmetric distribution, approximately log-normal, where the effect of changing the fragility is reflected in the average and variance of the local elastic constant values governing this distribution. The variance of the elastic constant fluctuations is found to be larger in the stronger glass-forming liquid. More surprisingly, we find that the Fourier transform of the shear modulus fluctuations in both the pure and the antiplasticized polymer materials exhibits a universal power scaling with the Fourier transform variable q in the glass state, suggesting that these glassy materials are in some kind of 'critical' state with regard to their elastic constant fluctuations. This observation is all the more striking given that we find no obvious evidence of large-scale density fluctuations in our simulated glass-forming liquids. We believe that these basic observations should be helpful in understanding the origin of the large transport property non-uniformities that arise in glass-forming liquids. Our results describing how changes in fragility affect changes in the elastic constant fluctuations can potentially provide insight into the scattering features associated with glasses, such as the Boson peak and anomalous low angle light scattering, as these features are commonly associated with elastic constant fluctuations.[31–38]

The remainder of our paper is organized as follows. Section 2 defines the model and the methods of calculation for the local and long-wavelength elastic constants. Sections 3 and 4 focus on the long and short wavelength elastic properties described above and we discuss some of their implications of these results in Section 5.

II. Methods

A. Model

The model employed in this work consists of a bead-spring polymer chain and smaller, spherical solvent molecules. It has been shown in our previous work that these small-solvent molecules antiplasticize the polymer material by decreasing glass transition temperature T_g, while simultaneously increasing both the shear modulus G and the density ρ in the glassy regime.[3–5,22,23,39,40] The polymer molecules were modeled as 32-segment chains, where each segment was connected *via* a stiff harmonic potential. Non-bonded interactions were taken into account using a Lennard-Jones (LJ) potential where both the energy and the forces were shifted at $r = r_{cut}$ such that they go smoothly to zero at r_{cut}. For both the polymer and the solvent molecules, the van der Waals interaction strength parameter ε in the LJ potential was taken to be unity, which prevents phase separation. For the pure polymer, σ_p was taken to be unity, while σ_S for the antiplasticizing additive was $0.5\sigma_p$, making the effective radius of the solvent molecules half that of the polymer monomers. The value of r_{cut} was $2.5\sigma_P$, and cross-interactions ε_{ij} and σ_{ij} are determined from the Lorentz-Berthelot rules, $\varepsilon_{PS} = (\varepsilon_P\varepsilon_S)^{1/2}$ and $\sigma_{PS} = 0.5\ (\sigma_P + \sigma_S)$. The mass of the polymer monomer was unity, while the mass of the solvent molecules equals 0.125, consistent with their relative volumes. The solvent concentration was 5% by mass (or ~30% by mol). The equilibrium bond length for the polymer chains was also unity, thus

creating an offset in the minima of the LJ potential and the harmonic bonded potential; it is this offset that promotes glass formation in these systems. All units in this work are reduced by the LJ parameters of the polymer monomers, *i.e.*, $T = k_B T^*/\varepsilon_P$, $E = E^*/\varepsilon_P$, where E is the energy and * represents an un-normalized quantity. Periodic boundary conditions were employed in all three directions.

Systems were equilibrated at $T^* = 1.0$ and independent configurations were generated at this temperature by performing MD simulations until the end-to-end correlation function had decayed for our systems. MD simulations were carried out at zero pressure for 10^7 time steps, after which the T was lowered in increments of 0.01 per 100 000 time steps to the desired temperature. Production runs were performed in the NPT ensemble at each desired temperature with $P = 0$. This protocol was employed to enable a direct comparison with experiments, which are performed at constant pressure rather than constant volume. All results presented below are averaged over five independent configurations, and uncertainties represent the standard error.

Many of the simulations described below involve temperatures below the glass transition temperature where equilibration is not possible. While our quench procedure yields a glass material with solid-like properties, an appropriate amount of caution must be taken in comparing such simulations directly to real materials. We have found that this procedure captures many of the qualitative aspects of real glass materials and we apply the method to explore basic properties of polymer glasses below; these issues are further elaborated in the Discussion section.

B. Calculation of isothermal compressibility and elastic moduli

Two sets of non-equilibration molecular dynamics calculations were performed to obtain the bulk mechanical properties. First, we performed uniaxial tension deformations at a constant true strain rate of 10^{-4} to obtain the Young's modulus E_Y, the deformation was applied to the x-direction while the y- and z-directions remained at zero pressure. The slope of the linear part of the stress–strain curve obtained from such a deformation is the Young's modulus; for the materials considered here, the stress response was approximately linear up to strains of 2%. Next, we performed isotropic tensile deformations at a constant true strain rate of 10^{-4} to obtain the bulk modulus K, which was taken as the slope of the stress *versus* the relative change in volume of the sample[41] for volume changes less than 1%.

We employ a combination of two techniques to obtain Poisson's ratio, ν. First, we can obtain ν directly from our uniaxial tension simulations as the ratio of the lateral strain to the tensile strain.[41] Our second approach began by assuming that our materials are isotropic and elastic so that all of the elastic constants are related to each other through the two Lamé coefficients, μ and λ. The Young's modulus expressed in terms of the Lamé coefficients is $E_Y = \mu[(3\lambda + 2\mu)/(\lambda + \mu)]$ and the bulk modulus is defined by $K = \lambda + 2\mu/3$. Thus, by directly measuring E_Y and K, we can calculate the Lamé coefficients and estimate the elastic properties such as the shear modulus, μ, or Poisson's ratio, $\nu = \lambda/(\lambda + \mu)/2$. Calculating ν through the Lamé coefficients represents our second measure of the Poisson's ratio. Both estimates of ν accord well with each other, giving us greater confidence in the mechanical property estimates.

Finally, the isothermal compressibility κ_T is calculated in the NPT ensemble by performing a long MD run and sampling the volume of the system at regular intervals. The isothermal compressibility is then defined as,[42]

$$\kappa_T = -\frac{1}{V}\left(\frac{\partial V}{\partial P}\right)_T = \frac{\sigma_V}{kTV} = \frac{\langle V^2\rangle - \langle V\rangle^2}{kT\langle V\rangle}, \quad (1)$$

where the angular brackets indicate an average over time.

C. Calculation of local shear modulus G and 'molecular stiffness' $1/\langle u^2\rangle$

The details of our method for calculating the local elastic constants have been presented elsewhere,[43,44] and here we recount only details required for understanding the present work. We begin by taking configurations from our lowest temperature, $T = 0.10$, and minimizing the energy of the system using the fast inertial relaxation engine[45] until the energy stops changing by more than 10^{-10} and the maximum force is smaller than 10^{-6}. Next, we calculate the stresses on each particle[46] before applying an infinitesimal strain to the system in the x-direction ($\varepsilon_x = 10^{-4}$) and minimizing the energy of the system again. Finally, we recalculate the local stresses on each particle; additionally we calculate the effective local strain for each particle ε_i using the method of Falk and Langer.[47] The local strain definition of Falk and Langer involves summing over the neighboring particles surrounding a central particle i. The local strain tensor for particle i is then defined as that which minimizes the local deviations from affine displacements. An analytical expression for the local strain tensor is available in ref. 47. We consider all particles within our LJ potential cut-off in the calculation of the local strain, and our results are insensitive to reasonable choices for this length. Using the changes in the local stress and the local strains, we define the local elastic constant as

$$C_{11,i} = \Delta\sigma_i/\varepsilon_i \quad (2)$$

where $\Delta\sigma_i$ is the change in stress on particle i. Note that the lateral directions are fixed at a constant length during this deformation; *i.e.*, we neglect any Poisson ratio effects during this calculation, although we expect these effects to be small given the small deformation we have applied. This explains why we denote the local shear moduli as $C_{11,i}$, consistent with the Voigt elastic constant notation.

In addition to directly measuring the local elastic constants by deforming our samples as described above, we have also considered the extent to which the local Debye–Waller factors can be used as a measure of local elasticity; we calculate them using two methods. First, in order to compare the Debye–Waller factors to the local elastic constants $C_{11,i}$, we utilize minimized and undeformed sample configurations to determine $C_{11,i}$ and we then performed MD simulations at very low temperatures ($T = 0.01$) to measure the average mean-squared displacement of each particle $\langle u^2\rangle_i$ after a characteristic average collision time, as in previous work.[28,48] The average collision time was specifically determined as the time that the velocity autocorrelation function first crosses zero, and corresponded to a time of approximately $t = 1.0$ in the reduced time units of both our systems. We note

that we perform these calculations at such a low temperature to facilitate comparison to the local elastic moduli, $C_{11,i}$.

Finally, at higher temperatures we employ the so-called "isoconfigurational ensemble" of Widmer-Cooper and Harrowell[30] to determine the Debye–Waller factors. In this technique, one begins several short MD calculations with all of the particles at the same starting location but with different initial velocities taken at random from a Gaussian distribution. This enables the calculation of local properties at higher temperatures where the diffusive nature of the particles would otherwise make it difficult to employ another method for calculating the local Debye–Waller factor.

III. Long-wavelength properties relating to elasticity and antiplasticization

A. Density and isothermal compressibility

As mentioned earlier, recent theoretical modeling of the fragility of glass formation by Dudowicz *et al.*[12] indicates that packing efficiency (referred to loosely as "packing frustration", see below) is at the origin of fragility variations of glass-forming liquids, and it is thus natural to start our discussion with how the addition of an antiplasticizer alters the ρ of the fluid, a basic measure of the relative efficiency of molecular packing. We show density data for both the pure and the antiplasticized polymer systems over a wide range of T in Fig. 1, ranging from near the onset temperature of the glass transformation regime T_A to temperatures well below T_g. (See Table 1 for a summary of the characteristic temperatures of glass formation that were previously estimated in these relatively fragile and strong polymer melts.[3–5] The definition of these characteristic temperatures is discussed at length in our previous papers[3–5] and we briefly summarize these definitions for completeness in Appendix A.) It is evident that the addition of antiplasticizer molecules tends to increase ρ, and thus enhances the packing efficiency of the material in the glass state; the effect is especially pronounced in the low temperature glass state. This is a widely recognized property of antiplasticized polymer melts and has led to numerous rationalizations of the antiplasticization effect in terms of simple free volume arguments. It is clear that the antiplasticizing additive is enhancing the average packing efficiency of the melt where the averaging is taken over large spatial scales.

Table 1 Characteristic temperatures of glass formation and their ratios for the pure polymer (PP) and antiplasticized polymer (AP) system. The run-to-run variation of the numerical estimates shown here and in the text of the paper is less than 2%

	PP	AP		PP	AP
T_c/T_g	1.25	1.40	T_A	0.59	0.51
T_c/T_0	1.32	1.52	T_c	0.42	0.34
T_A/T_c	1.33	1.46	T_g	0.37	0.26
T_A/T_g	1.71	2.04	T_0	0.36	0.23
T_A/T_0	1.76	2.22			

Fischer and co-workers have emphasized 'free volume' or density fluctuations in their discussions of the antiplasticization effect,[49] based on the heuristic notion that particle mobility mainly reflects the amount of 'free volume' allowed for particle motion. The magnitude of density fluctuations at equilibrium is appropriately quantified by the isothermal compressibility, κ_T. We note that κ_T is a central quantity in Schweizer's generalized mode-coupling theory of the dynamics of glass formation,[50–52] providing another motivation for investigating how antiplasticizing additives alter this basic thermodynamic property.

Fig. 2 shows the effect of the antiplasticizer on κ_T over a wide T range as in the ρ data. As might be expected from our discussion of the change in density with the addition of the antiplasticizer, we see that κ_T is reduced by the antiplasticizer additive at all temperatures. The surprising aspect of the observed trend is that the effect of the additive becomes larger with increasing temperature, in contrast to the density data where the difference between the plasticized and antiplasticized systems progressively diminishes with increasing T. Apparently, the average density and the density variance behave somewhat differently with the addition of the antiplasticizer additive. Adding the antiplasticizer results in a more dense material, but the change in density is modest (a few percent). The antiplasticizers can appreciably modify the small-scale density fluctuations, which lead to appreciable modifications of the fragility of the polymer. Fischer *et al.* have also shown how small molecule additives can decrease the compressibility of a polymer glass.[49]

In a previous paper,[3] we examined how the local free volume, as measured by the local Voronoi cell volume associated uniquely with each particle, correlates with local particle

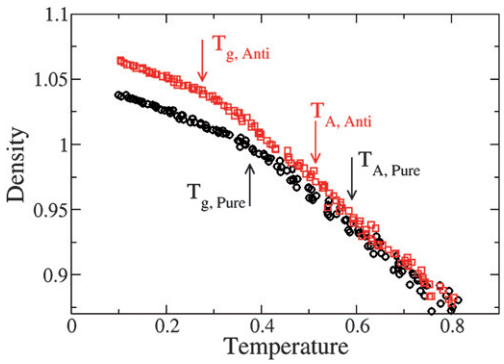

Fig. 1 Density as a function of temperature for the pure polymer (circles) and the antiplasticized polymer (squares) calculated by cooling from $T = 0.8$ to $T = 0.1$ at a rate of $\Delta T/\delta t = 10^{-4}$.

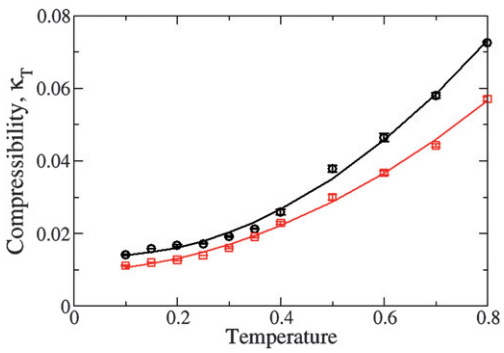

Fig. 2 Compressibility as a function of temperature for the pure polymer (circles) and the antiplasticized polymer (squares). The lines are a guide to the eye. All error bars represent the standard errors amongst the quantities measured in five independent simulations.

mobility. That work indicated, as found previously,[28] that this intuitively appealing and widely believed relationship between local free volume and particle mobility does not really hold. We tried to gain further insight into this surprising finding by examining local density fluctuations in the pure polymer and antiplasticized polymer melts. That effort was not successful, and any differences in the rather uniform local packing density in terms of fluid cavity structure were hard to discern, although we do not mean to imply that density fluctuations do not exist. Rather, any such fluctuations must be operative on small spatial scales.[53] This negative finding should be kept in mind in our discussions below of the elastic constant fluctuations in these polymeric fluids where large-scale elastic constant fluctuations are rather conspicuous in these same materials. Evidently, there is no obvious link between free volume fluctuations and elastic fluctuations in the melt either.

B. Shear modulus G, bulk modulus K and Poisson ratio ν

The bulk modulus K and shear modulus G are measures of the forces required for isotropic and shear deformation of these materials, while the Poisson ratio provides a measure of the relative magnitudes of these basic measures of material stiffness. A general stiffening of a material, while T_g simultaneously decreases, is often taken as a defining property of antiplasticizing additives and we can expect elastic moduli to be informative about the fragility of glass formation. Enhancing the packing efficiency (increasing the density and decreasing κ_T) might be expected to lead to a straightforward increase in the material rigidity, but we find that this trend is more subtle than one might expect. Fig. 3 shows the T dependence of the Young's modulus E_Y (related to the shear modulus by a simple transformation, see below). The antiplasticized polymer is indeed stiffer in the glass state, but becomes softer at a temperature comparable to T_g of the pure polymer melt, an effect seen in many real experimental systems.[6,7] This temperature crossing phenomenon in the effect of the antiplasticizer on G also shows up in the bulk modulus K and Fig. 4 shows corresponding data for K over a wide T range. Again we see a tendency towards temperature crossing of the properties of the pure and antiplasticized polymer melts, although the crossing temperature is closer to the temperature T_c of the pure polymer melt (see Table 1) for K.

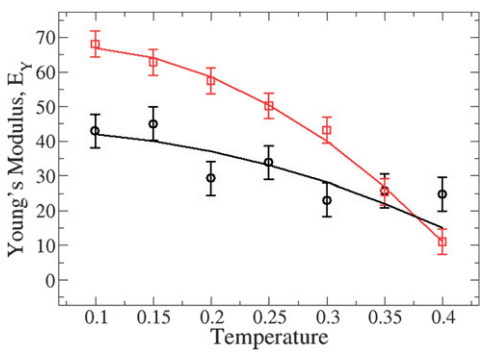

Fig. 3 Young's modulus Y as a function of temperature for the pure polymer (circles) and the antiplasticized polymer (squares). The Young's moduli Y cross each other near $T = 0.35$, near T_g of the pure polymer. The lines are a guide to the eye and do not represent a fit to any specific functional form.

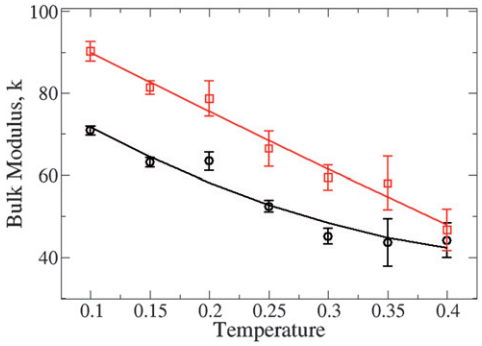

Fig. 4 Bulk modulus K as a function of temperature for the pure polymer (circles) and the antiplasticized polymer (squares). K apparently crosses at a higher temperature than Y. The lines are a guide to the eye and do not represent a fit to any specific functional form.

We also observe the temperature crossing effect in the Poisson ratio ν, a crucial processing variable for polymeric materials. (The progressive increase in ν with T indicated in Fig. 5 for both the pure and the antiplasticized polymer materials is a ubiquitous property of glass-forming liquids.[54] It is also apparent that the lower packing efficiency of the antiplasticized polymer melt in the glass state is reflected in a lower relative ν value. However, above T_g, the antiplasticized polymer fluid has an appreciably larger value of ν, approaching its limiting value of 1/2 appropriate for an ideal incompressible elastic medium. (In the high temperature regime, we are discussing high frequency moduli which are conveniently measured by Brillouin or other light scattering method.) Evidently, trends between fragility and ν, determined from mechanical measurements in the glass state ($T < T_g$), could be quite different from Brillouin scattering and other estimates obtained at T above T_g. It is thus essential to specify the

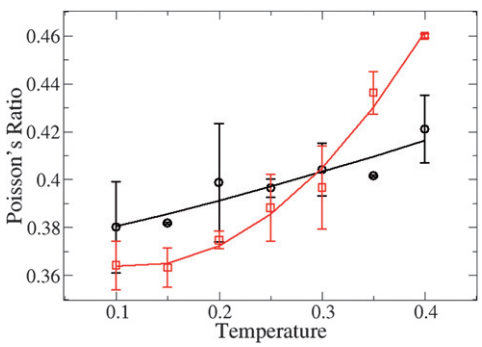

Fig. 5 Poisson's ratio ν as a function of T for the pure polymer (circles) and the antiplasticized system (squares). These quantities are derived for each system based on the Lamé coefficients extracted from the calculations of the Young's modulus and the bulk modulus above. The Poisson's ratio crosses near $T = 0.30$, similar to the crossing temperature ($T = 0.35$) found for E_Y. For comparison, the glass transition temperature of the pure polymer melt is estimated to be about $T = 0.36$ (see Table 1). The lines are a guide to the eye and do not represent a fit to any specific functional form. The lines are a guide to the eye and not a fit to any functional form.

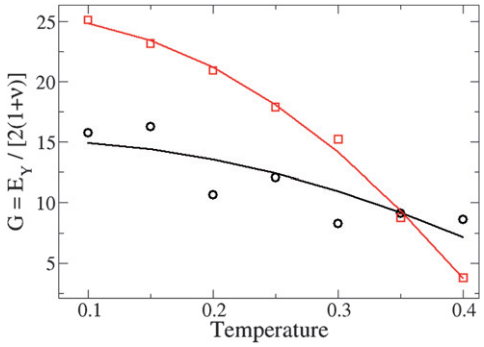

Fig. 6 Shear modulus G as a function of temperature for the pure polymer (circles) and the antiplasticized system (squares). We determine G from E_Y and ν and the formal equation relating these quantities discussed in the text. The G curves again cross near T_g. The lines are a guide to the eye and not a fit to any functional form.

temperature range involved in any discussion of the trends in ν with fragility.

The combination of E_Y and K allows the calculation of the Lamé coefficients, including the shear modulus G as a function of T. Fig. 6 shows G obtained in this way and we again observe the temperature crossing of G as a function of T. The crossing occurs near T_g, as in the case of ν. Reassuringly, this method of estimating $G(T)$ is quite consistent with our previous estimate of G for the same system from a simulation of a small oscillatory shear deformation of the pure and antiplasticized polymer materials.[3]

IV. Determination of local elastic constants and their spatial distribution

A. Local elastic constants

A value of $\nu = \frac{1}{2}$ is characteristic of an ideal homogeneous incompressible elastic medium that locally deforms affinely with a macroscopic deformation, and the progressive reduction of ν of cooled polymer melts from this value suggests a progressive growth of material non-uniformity of some kind and a corresponding progressive growth of non-affine local deformation associated with these material non-uniformities in the glass state. There have been numerous reports of the progressive growth of dynamic heterogeneity in supercooled liquids and colloidal particle systems that are consistent with this general trend[54] and Zondervan *et al.*[55] have claimed to have found direct experimental evidence of the existence of large-scale tenuous elastic structures within highly supercooled model glass-forming liquids through careful rheology measurements, despite the lack of convincing scattering evidence for such structures. We thus examine the elastic constant heterogeneity in these model glass-forming liquids to determine how varying fragility affects this aspect of glass-forming liquids.

We obtain estimates of the local elastic constants within the polymer glass by following the methods described in ref. 43 and 44, where the material is subjected to a macroscopic deformation and the local elastic constant is inferred from the extent of the local deformation that arises from the macroscopic deformation where Hooke's law is assumed to locally apply.[27] Notably, fluctuations in the local stress in the medium will be registered as changes in the local modulus in our treatment so one may also think of the variations we observe as being reflective of local stress variations in the material. Indeed, the general existence of local stress fluctuations has been noted before as a basic feature of glass-forming liquids.[56] This alternate interpretation of the elastic constant fluctuations should be kept in mind when we refer to the apparent value of the 'local' elastic constant.

Fig. 7a and b show a color map indicating the variation of the local elastic constants C_{11} in the pure and antiplasticized polymer, respectively, in the low temperature glass state. Red denotes regions of relatively high shear modulus, while blue represents unstable regions having a formally negative local C_{11}. The color map provides a relative intensity level for these elastic constant variations. We refer to the light blue domains as the 'frustrated regions'. We can expect that deformation to be highly non-affine in these regions of frustrated packing and we have verified that this is the case. The molecules in these frustrated regions can be figuratively imagined as something like a jack-in-box toy, where an application of a small deformation can cause a reactive deformation in the opposite direction from the applied force and

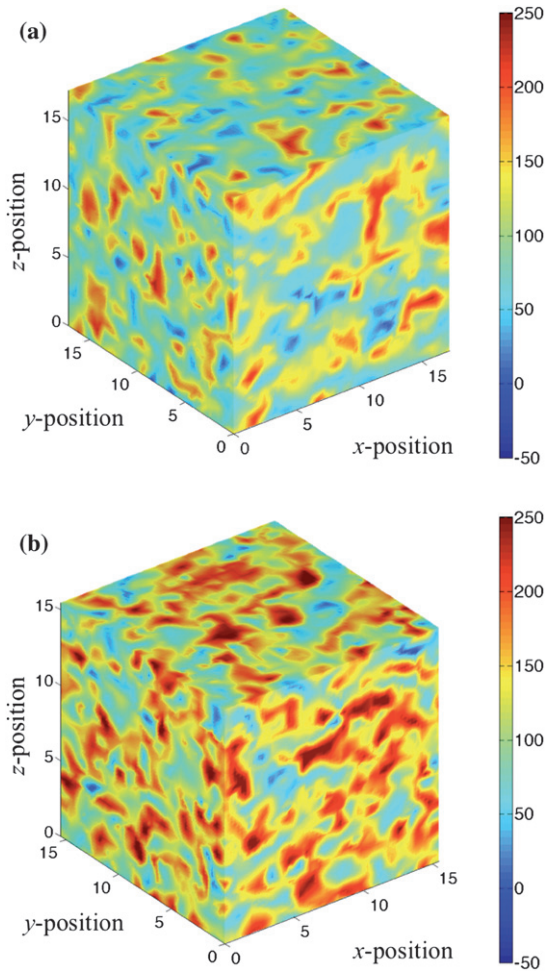

Fig. 7 Color maps of the local elastic constants (C_{11}) for the pure polymer (a) and the antiplasticized system (b). The dark blue domains correspond to domains of negative C_{11} while the dark red domains correspond to extraordinarily stiff domains. The color map scale is the same for both images (color online).

a decrease in the local stress with increasing strain.[27] It is known that the incorporation of materials having this odd non-equilibrium property can result in materials of extraordinary toughness[57,58] and other unique properties.[59] In our systems in the glassy state, the lifetime of these frustrated domains is longer than the time scales of our simulations. We see that the high stiffness regions clearly form a percolating network in the elastic constant map of the antiplasticized glass material (Fig. 7b). This is true even though the antiplasticized system is denser and presumably more uniform in density than the pure polymer system. We did not expect the stronger glass former to exhibit much stronger fluctuations in its local elastic constants, but this phenomenon (anticipated by Novikov *et al.*[60]) certainly accords qualitatively with the observation of a more intense Boson peak in strong glass-forming liquids[5,36,61] and the association of this scattering feature with strong elastic constant fluctuations.[31–36] At any rate, the fluctuations in the local elastic constants are appreciably different in these model fragile and strong glass-forming liquids.

An examination of the distribution of the local elastic constant values (without regard to region location) reveals some interesting regularities. Fig. 8 shows the distribution of C_{11} for the pure polymer and antiplasticized systems, where we find that both distribution functions obey a shifted log-normal distribution (*i.e.*, we fit our data to a log-normal distribution after shifting the x-axis such that all values are positive and then remove the shift on both the raw data and the fit function). The average value of C_{11} is larger in the antiplasticized system, and the range of C_{11} fluctuations is also larger. The variance σ_G of the shear elastic constant fluctuations provides a measure of the elastic constant fluctuations that serves this effect and this quantity equals 57 and 84 for the pure, fragile polymer and the strong antiplasticized system, respectively. In previous work, the variance of the shear modulus fluctuations was reduced through the introduction of nanoparticles into a polymer matrix, an effect that Starr and Douglas[63] have established to be associated with making glass formation process more fragile. Thus, while there seems to be some regularity in the distribution of the local elastic constant distribution, the mean and variance of these distributions are significantly influenced by fragility.

Why should a greater variance in the shear modulus fluctuations be expected in glasses in which molecular packing is more efficient? We suggest that the greater packing efficiency actually engenders a stronger seizing or 'jamming' of the material in the glass state. This effect should be kept in mind with respect to the term 'packing frustration'.

The spatial distribution of the shear modulus fluctuations is also informative about the nature of elastic constant fluctuations in glasses and the variation of these fluctuations with fragility. Initially, we expected a characteristic length scale associated with the elastic constant fluctuations that would determine the Boson peak frequency, as expected from some models of this phenomenon.[64,65] Additionally, recent molecular simulations have suggested a characteristic length scale in the non-affine displacement fields and we initially thought that this scale might be identified with a corresponding length scale in the elastic constant fluctuations.[32,33] We were surprised to find, however, that such a relation does not exist for the elastic constant fluctuations. The Fourier transform $I(q)$ of the elastic constant fluctuations shown in Fig. 9 leads to an extraordinary and unanticipated result; $I(q)$ scales in near perfect proportionality to q^{-2}. This type of scaling is reminiscent of the low angle scattering intensity of critical fluids or magnetic systems near their critical point for phase separation or ordering, respectively.[66] The antiplasticized polymer material (*i.e.*, stronger glass former) is distinguished only by having a larger prefactor in this general scaling relation, reflecting the greater intensity of the elastic constant fluctuations in the stronger glass-forming material. The elastic constant fluctuations are thus characterized by significant changes in amplitude and variance with fragility, but the distribution of elastic constant values and their distribution in space are suggested to be universal in glass-forming liquids. Again, we stress that our simulations indicate that nothing particularly interesting is apparent in the density fluctuations of these materials. The 'critical' behavior of the glass state involves the elastic properties rather than density fluctuations, as in the case of liquid–vapor phase transitions. Fischer and co-workers[49,67] and more recently

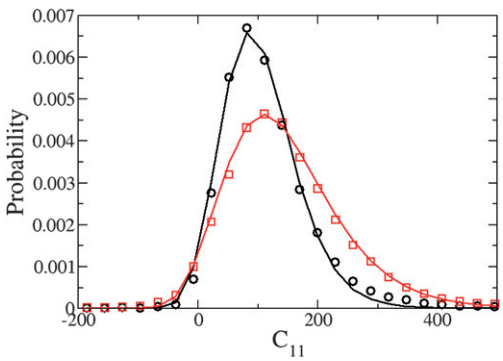

Fig. 8 Distribution of local elastic modulus values for the pure polymer and the antiplasticized system materials. The solid lines are a fit to the shifted log-normal distribution. This distribution is conspicuously similar to the prediction for the distribution of localization lengths in an amorphous solid.[62] A near log-normal distribution is also found for the distribution of the free volume (Voronoi volume) at all temperatures for a wide range of glass-forming liquids.[28]

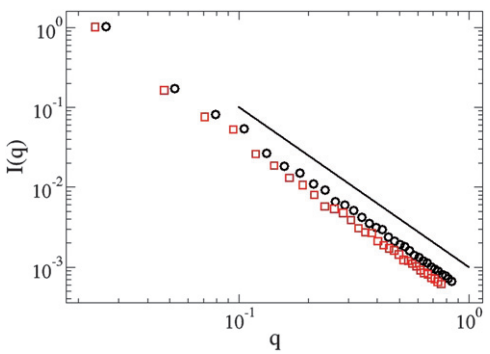

Fig. 9 Spatial Fourier transform of the elastic constant map shown in Fig. 7. Pure polymer is denoted by circles and the antiplasticized system by squares. The solid line indicates the scaling relationship, $I(q) \approx q^{-2}$, for comparison with the data. The prefactors for the scaling relationship are 6.8×10^{-4} and 5.5×10^{-4} for the pure polymer and antiplasticized system, respectively.

Patkowski *et al.*[68,69] found significant light scattering in model glass-forming liquids, consistent with the scattering light intensity $I(q)$ scaling as q^{-2}, but these observations were interpreted in terms of density fluctuations. In the belief that local free volume governs local mobility, Fischer *et al.* have also ascribed antiplasticization to changes in the variance of density fluctuations.[49] Elastic constant fluctuations should be accompanied by dielectric constant fluctuations through a stress optical relationship, and we suggest that the anomalous light scattering of glass-forming liquids might have its origin in elastic constant fluctuations in the medium. Other optical effects, such as the 'red edge effect' relating to the shifting of fluorescence optical probe data, have been attributed to the dynamic heterogeneity of glass-forming liquids, and ionic fluids in particular.[70] Rheological measurements on model glass-forming liquids have been interpreted as providing direct evidence of extended, delicate solid-like network structure within supercooled liquids.[55] Our simulation observations are broadly consistent with these measurements.

B. Local Debye–Waller factor $\langle u^2 \rangle$ as a local force constant

The mean-square particle displacement $\langle u^2 \rangle$ represents a kind of compliance and $k_m \equiv k_B T/\langle u^2 \rangle$ can be interpreted as a molecular force constant or local elastic constant[2,29,71] governing local particle localization in the glass state. The 'Debye–Waller factor' $\langle u^2 \rangle$ is a particularly interesting property since it can be measured by neutron scattering and because previous work has shown that variations in this quantity correlate with particle mobility in the supercooled liquid state.[30]

Fig. 10a plots the mean-squared displacement $\langle r^2(t) \rangle$ as a function of time at three different temperatures. Fig. 10b shows the average value of $\langle u^2 \rangle$ as a function of T for both the pure and the antiplasticized polymer fluids; $\langle u^2 \rangle$ was taken as the value of $\langle r^2(t) \rangle$ at $t = 1.0$, as described in ref. 28 and 48 As in the case of the long-wavelength determination of G, $\langle u^2 \rangle$ for the pure and antiplasticized polymer melts as a function of T seems to exhibit a crossing at low T, in this case occurring near the VFTH temperature T_0 (see Table 1 and Appendix A) of the pure polymer. However, the small magnitude of $\langle u^2 \rangle$ in the glass regime makes it difficult to resolve this crossing behavior and the reciprocal of $\langle u^2 \rangle$ tends to be somewhat noisy. We then expect the observation of a crossing of $\langle u^2 \rangle$ to be more difficult to observe than the crossing of G in antiplasticized materials, a behavior confirmed in a recent experimental study.[2]

We obtain further evidence of this correspondence between the local elastic modulus $C_{11,i}$ and $\langle u^2 \rangle$ by looking at the distribution of $1/\langle u^2 \rangle$, shown in Fig. 11. The spatial distribution of $1/\langle u^2 \rangle$ was illustrated in a previous paper,[3] where an image similar to the elastic constant map in Fig. 7 was reported. The trends observed for $1/\langle u^2 \rangle$ and $C_{11,i}$ at a local scale are also quite similar. The advantage of this relationship is that $\langle u^2 \rangle$ for a time shorter than the structural relaxation can be estimated above T_g, which allows for a well-defined discussion of local transient stiffness fluctuations in the fluid in the liquid state.

We briefly illustrate this last point through a consideration of molecular stiffness ($1/\langle u^2 \rangle$) maps made at both a relatively high and a low relative temperature. In our former study, we compared $\langle u^2 \rangle$ for the same antiplasticized and pure polymer models as considered in the present paper. We observe in

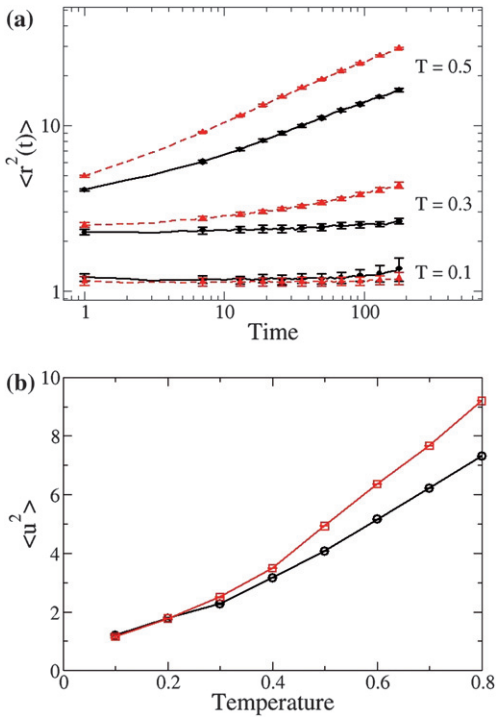

Fig. 10 (a) Mean-square displacements as a function of time at three different temperatures for the pure polymer (solid lines with filled circles) and the antiplasticized polymer (dashed lines with filled triangles). (b) Debye–Waller factors $\langle u^2 \rangle$ as a function of T for the pure polymer (circles) and the antiplasticized polymer determined from the mean-squared displacement, $\langle u^2 \rangle$. The Debye–Waller factor $\langle u^2 \rangle$ is determined computationally by the condition, $\langle u^2 \rangle \equiv \langle r^2(t) \rangle$ at $t = 1.0$.[28] Solid lines are a guide to the eye. $\langle u^2 \rangle$ curves apparently cross near $T = 0.2$, near T_0 of the pure polymer.

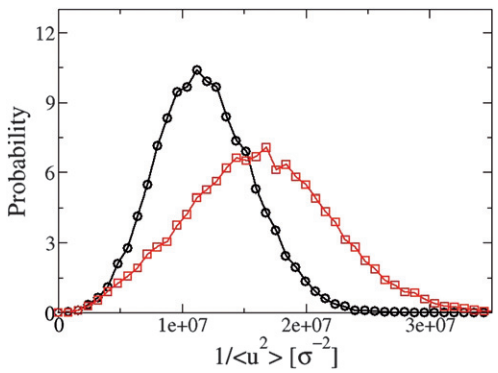

Fig. 11 Distribution of $\langle u^2 \rangle$ in the glass state ($T = 0.01$) for plasticized and pure polymer materials. Color designations of data for the antiplasticized and pure materials are the same as in Fig. 7 and 8. Solid lines are a guide to the eye.

Fig. 11 that $1/\langle u^2 \rangle$ fluctuations exist even at relatively high temperatures that well above T_g and that these fluctuations exhibit a similar peaked distribution as in the case of the shear modulus fluctuations (see Fig. 7), although this distribution appears more Gaussian than log-normal in nature. We also found that the variance σ_u of the molecular stiffness

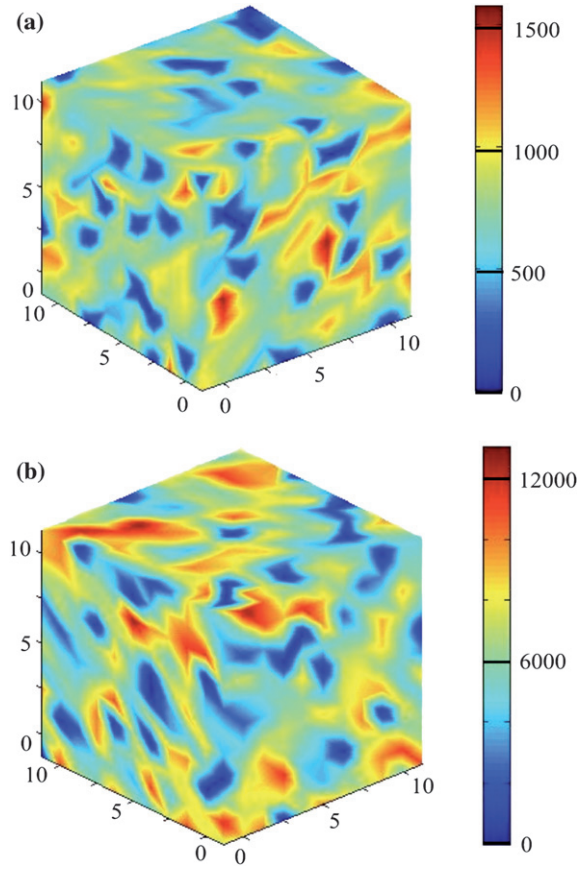

Fig. 12 Color maps of the local values of the molecular stiffness $1/\langle u^2\rangle$ for the pure polymer at $T = 0.60$ ($T/T_g = 1.62$) (a) and $T = 0.15$ ($T/T_g = 0.41$) (b). The red regions correspond to domains of large $1/\langle u^2\rangle$, while the blue domains correspond to a small stiffness, $1/\langle u^2\rangle$. Note that the color scale is different in each figure.

fluctuations is again larger in the case of the stronger glass-forming liquid, *i.e.*, σ_u (pure) $= 3.9 \times 10^6 \pm 0.1 \times 10^6$ *versus* σ_u (antiplasticized) $= 6.0 \times 10^6 \pm 0.1 \times 10^6$.

Fig. 12 also shows that there is a little discernible change in the percolative characteristics of the stiff regions with temperature in the high and low temperature as shown in Fig. 12a and b. Evidently, it is the lifetime of the dynamically heterogeneous regions that is most affected by a change in temperature. This observation is of relevance to speculative arguments that attribute vitrification to some kind of percolation transition of rigid or fluid-like regions.

V. Discussion

Due to the dramatic differences in the time scales and cooling rates accessible to molecular simulations and experiments, the ability of simulations to reproduce experimental phenomena associated with the glass state is not obvious *a priori*. We therefore begin our discussion by establishing the ability of molecular simulations to reproduce properties associated with the glassy state and the glass transition. We focus on several of our own studies in which molecular simulations reproduce the trends observed in experiments on glassy materials. For example, quantitative agreement between neutron scattering experiments and the Debye–Waller factors $\langle u^2\rangle$ for antiplasticized sugars well below T_g has been reported recently,[44,72] and non-equilibrium molecular dynamics simulations reproduce the temperature dependence of the dynamic mechanical properties from well below T_g to slightly above T_g.[73] Other non-equilibrium studies, such as those examining the changes in the mobility of glasses during deformation, agree remarkably well with experiments.[74,75] Of particular relevance to this work, the models considered here have been demonstrated to reduce the effects of confinement on T_g,[5] in accord with the experiments of Ellison *et al.*[76] Taken together, our prior studies give us confidence that our coarse-grained molecular modeling is sufficient to gain insight into the properties of the glass-forming liquids, despite the necessarily short time scales accessible to simulation relative to experiments on glass-forming liquids.

The addition of an antiplasticizer additive to a polymer melt influences molecular packing and leads to numerous changes in material properties through its effect on the glass transition in these materials. In particular, many 'amorphous' polymers (*e.g.*, polystyrene) that are not readily subject to crystallization are 'fragile' glass formers in that their transport properties such as the viscosity, diffusion coefficient and structural relaxation time vary strongly with temperature. In relative terms, the addition of antiplasticizer additives renders these polymer materials stronger glass formers.[3–5] These changes in fragility with the addition of antiplasticizer allow us to investigate how the elastic properties of the polymer melt, and other glass-forming liquids, depend on fragility. Glass-forming liquids at low temperatures possess a rather uniform density, but these materials are apparently highly non-uniform in the glass state with respect to particle mobility and material stiffness. We thus examined the nature of elasticity in the long-wavelength limit, where the elastic constants are thermodynamic properties of the material, separately from the local elasticity at the nanoscale.

Our examination of the long-wavelength thermodynamic properties of our model fragile (pure polymer) and strong (antiplasticized) polymer systems indicates that the antiplasticizer increases the packing efficiency of the material, as directly evidenced by an increase in density and a reduction in the isothermal compressibility where the effect seems to be operative at all temperatures. The effect of the antiplasticizers and the corresponding change of fragility have a subtle influence on the temperature dependence of the elastic moduli, however. The shear G and bulk K moduli are larger at temperatures well below the glass transition temperature, as one would generally expect from an enhancement of molecular packing by an additive; this trend inverts upon heating and the antiplasticized system actually becomes softer at elevated temperatures, as observed experimentally.[6,7,77,78] The crossing temperature for G was found to occur near the glass transition temperature of the pure polymer melt, while this temperature occurs at a higher temperature for K. The Poisson ratio ν of the antiplasticized material becomes smaller in the glass state relative to the pure polymer melt and also exhibits a crossing temperature, a fact of relevance to recent attempts to correlate to the fragility of glass formation.[24,25,31,36] The crossing phenomenon means that the characteristic stiffening associated with antiplasticization has a limited temperature range in which it is observed, implying that such additives could readily be confused with plasticizer additives if measurements are

only performed in the high temperature polymer melt state where the additive softens the material.[2,77] The influence of water on many biological materials[78–81] and polar polymeric materials such as epoxies used in coatings, *etc.* provides numerous practical examples of a temperature dependent antiplasticization effect, where moisture can render everyday materials (food, paper) relatively hard, brittle and impermeable, and alter their physical aging properties considerably.[82–84]

Other studies have shown that the temperature crossing phenomenon in the elastic moduli is also reflected in high frequency or secondary β relaxation processes of the material. In particular, the Johari–Goldstein[85] relaxation process also crosses at a temperature that appears to be in the proximity of the glass transition temperature of the pure glass-forming liquid.[2] A slowing down of the high frequency dynamics thus accompanies the enhanced stiffness of the antiplasticized material and high frequency measurements provide a convenient means of locating the 'antiplasticization temperature' where the stiffening effect initiates in the mixture. This stiffening effect has recently been shown to be useful in the preservation of protein drugs[1] and has promise for many other technologies such as the stabilization of nanoimprinted polymer structures and the lithographically etched substrates.[86–88] Antiplasticizer additives have already proved their value in the formation of scratch resistant films for coating photographs and other images.[89]

An understanding of the dramatic changes in the long-wavelength elastic properties of polymer melts with antiplasticizer additives requires a consideration of the non-uniformity of the elastic properties at a nanoscale or molecular scale. Just as the dynamics of cooled glass-forming liquids can be understood from the development of progressively cooperative molecular motion upon cooling and emergent dynamic heterogeneity, the elastic constant values reflect elastic heterogeneity that becomes quenched into the glass as the lifetimes of the heterogeneities observed at higher temperatures become extremely long. The slow growth of this structure can be expected to account for physical aging and the modification of this structure by deforming or otherwise perturbing the glass is no doubt relevant to polymer processing and for understanding the plasticity of polymer materials. We thus investigated this local elastic heterogeneity to determine basic aspects of its structure and how fragility alters its character.

First, we constructed a map of the local shear elastic constant by macroscopically deforming the pure and antiplasticized materials and assigning a local elastic modulus to each particle in the material; we subsequently averaged over local cubic volumes to obtain a map of the local elastic constant fluctuations of the material. This procedure revealed that the more efficiently packed antiplasticized material exhibits much more intense elastic constant fluctuations than the pure polymer melt. The variance of these fluctuations was also broader implying that these materials are more elastically heterogeneous than the pure polymer melt. Another evident feature in the elastic constant maps is the presence of unstable fluid regions that formally have a negative local shear modulus, such regions occupying an appreciable amount of the pure polymer material. The local mobility has been shown to be higher in the regions with a modulus near zero,[43] an effect is of importance to protein preservation in fragile high glass transition sugars such as trehalose, where this relatively high local mobility could translate into tendency for proteins to degrade, despite being in the glass state where the rate of large-scale diffusion is very low. Despite these differences in the average and variance of the local elastic modulus in the pure and antiplasticized polymer materials, we found that the distribution of the elastic constants (without regard to location of the coarse graining cells in space) is nearly universal, taking a form that is approximately a shifted log-normal distribution for the shear modulus, G and a Gaussian function for the 'molecular stiffness', $1/\langle u^2 \rangle$.

One of the most striking observations that we have made about the local elastic constant fluctuations in our model glass materials concerns the nature of the spatial correlations in these fluctuations. We had expected to find a characteristic scale in these fluctuations that we could correlate with the Boson peak frequency, but instead we found that the elastic constant fluctuations form a fractal structure or more specifically a Fourier transform $I(q)$ of our elastic constant map revealed a universal power-law scaling, $I(q) \approx q^{-2}$, where the prefactor is larger for the stronger, antiplasticized glass.

Evidently, the glass is in a kind of critical state with regard to its elastic constant fluctuations, and $I(q)$ exhibits a scaling with q similar to the scattering intensity of fluids near their critical point for condensation or phase separation. As best as we can tell, this critical scaling is not accompanied by a corresponding scaling in q describing density fluctuations in the glass and, indeed, we find our model glasses to be remarkably homogeneous in terms of its density at the nanoscale and larger. Recent high resolution rheological and single molecule relaxation measurements have claimed to have found evidence for such an elastic network structure in glass-forming liquids at low temperatures.[90,91] There is also evidence for such large-scale heterogeneity from fluorescence measurements on certain ionic fluids.[92]

The power-law scaling of the elastic constant fluctuations was unexpected and we can only offer tentative rationalizations of this important phenomenon. It seems highly plausible that this fractal structure represents an extension of the dynamical heterogeneity structure observed in previous simulations restricted to higher temperatures where the fluid is equilibrated. In particular, the excessively mobile particles were found to form clusters having a fractal structure with a fractal dimension near 2,[14,18] and particles having excessively low mobility correspondingly also formed highly extended clusters[93,94] where the immobile particles are associated with a dense packing geometry inconsistent with a macroscopic crystal.[95,96] In this picture, the mobile particle regions are akin to the grain boundary regions of polycrystalline material except these regions occupy a large fraction of the glass-forming liquid, and the ordered regions are not proper crystals having a long-wavelength translational symmetry. Previous simulations have shown a tendency of the average mass of the mobile particle clusters (the immobile particle has not been so well characterized) to diverge as the crossover temperature T_c is approached,[97] and similar percolation behavior can be expected for the immobile particle regions.

It seems quite plausible that the emergence of fractal network of high stiffness within a soft background is the direct extension of the dynamic heterogeneity phenomenon observed in previous simulations, where the fractal network below the glass transition temperature is effectively a frozen structure rather than

a dynamically fluctuating structure found in the higher temperature fluid simulations. A fractal dimension of 2 is the exact fractal dimension of equilibrium branched polymer ('lattice animals') in three dimensions or equivalently a random branched polymer network formed under equilibrium conditions with strong repulsive excluded volume interactions.[98] An alternate possibility relates the emergence of the amorphous solid state.[99] It is established that such materials spontaneously exhibit strain fluctuations at equilibrium whose mean-square value scales as q^{-2}.[100] Such strain fluctuations translate the formal application of Hooke's law locally to spontaneous local stress fluctuations in amorphous solids. It is possible that the local 'elastic constant' fluctuations that we report actually reflect these local stress fluctuations. If so, this would naturally explain the universality that we observe in the elastic constant correlations in the glass state.

The nanoscale elastic constant heterogeneity is germane to the macroscopic elastic properties because this property engenders local strain non-uniformities in the deformed material. The resulting non-affine nature of local displacements within the material can qualitatively explain the drop of the Poisson ratio upon cooling as the contribution of the non-affine regions becomes more prevalent. The magnitude of this effect is clearly modulated by the antiplasticizer, and more generally fragility, because this property controls the magnitude and variance of the elastic constant fluctuations. Fluctuations in local packing and the corresponding prevalence for non-affine local deformation are also prevalent in granular materials[22,101–103] and polymer foams[104,105] and the Poisson ratio in such materials can become quite small. Basically, we can imagine that the local mechanical property heterogeneity of glasses makes these materials effectively 'granular' in nature and the changes in the elastic constant can be qualitatively understood from this general viewpoint.

It should be appreciated that our observation of apparently 'fractal' elastic constant fluctuations is limited to the scales of our simulations (our box lengths are approximately 12σ) and some natural cut-off scale likely exists at larger scales where the material can be expected to behave more as a continuum elastic material. Indeed, Barrat and co-workers[106] have identified a cut-off scale in two dimensions on the order of 40σ (which is on the order of 40 nm if we take σ on the order of a nm). This conclusion was based on an examination of the degree of affineness of local deformations in the glassy material, following a large-scale deformation, and this analysis revealed the existence of complex vortex-like structures, associated with the local non-affine character of the deformation field, having a characteristic size of the order of 40σ in 2D. Unfortunately, the size of our 3D simulations does not allow us to probe such a large-scale phenomenon and it is entirely possible that a scale consistent with the simulations of Barrat and co-workers[106] exists beyond which the power-law elastic constant scaling that we observe breaks down, reflecting a transition to an effectively continuum elastic material at large length scales. We plan to explore this potential crossover in the elastic constant scaling in the future since this scale is of obvious potential significance for understanding the onset of finite-size effects of glass-forming liquids such as T_g, the shear and bulk moduli of the material, *etc.* A scale of 40σ is quite consistent with numerous observations of the finite-size onset scale for glass-forming liquids.

As an adjunct to our investigation of the local elastic constant variations in our pure and antiplasticized materials, we also considered its truly molecular counterpart, the Debye–Waller factor, which provides a measure of the molecular force constant locally confining particles in the condensed state at low temperatures. In particular, the ratio $k_BT/\langle u^2\rangle$ can be identified as force constant within a simple harmonic localization model and it is natural to compare this quantity to the local G. Our simulations show that the distribution of values similarly follows an approximately log-normal distribution and exhibits a very similar network structure in the glass state as G. This not only supports the common experimental interpretation[29] of $1/\langle u^2\rangle$ as some kind of local or molecular elastic constant, but also opens up an opportunity to explore the formation and nature of the network of elastic constant fluctuations at higher temperatures where G cannot be determined. We look forward to considering this problem in future work.

Appendix A: characteristic temperatures of glass-formation

The dynamics of glass-forming liquids is characterized by a number of temperatures, which in decreasing order include T_A (demarking the onset of the cooperative atomic motion), a crossover temperature T_c (separating high and low-T regimes of glass formation), the glass transition temperature T_g (below which aging and other non-equilibrium behavior are overtly exhibited), and finally T_0 (characterizing the 'end' of the glass transformation process).[12] T_A is experimentally defined as the T at which the Arrhenius temperature dependence of τ no longer holds.

A variety of structural relaxation processes can be chosen to examine the rate of structural relaxation in glass-forming liquids. The bond autocorrelation function $\psi(t)$ provides a particularly convenient estimate of the relaxation time in our model polymers, and previous work has shown that this quantity gives essentially the similar τ estimates to those obtained from the dynamic structure factor.[19] In particular, τ is defined in the present work as the time where $\psi(t)$ has decayed to $1/e \approx 0.368$.

Based on the entropy theory of glass formation,[12] the apparent activation energy $E_a(T)$ of glass-forming liquids follows a universal quadratic T dependence, $E_a(T)/E_a(T \to T_A) \approx 1 + C_0(T/T_A - 1)^2$, where C_0 and T_A are determined by fitting to relaxation time τ data for of pure and antiplasticized polymer melts to this relation.[3]

To estimate the other characteristic temperatures in Table 1, we fit our τ data to the Vogel–Fulcher–Tammann–Hesse (VFTH) equation,

$$\tau = \tau_0 \exp\left(D\frac{T_0}{T - T_0}\right) \tag{A1}$$

where T_0 is a temperature at which τ formally diverges upon extrapolating eqn (A1) to low temperatures. T_g is determined by the simple criterion that the structural relaxation time τ equals 100 s. The estimation of T_g and T_0 from molecular dynamics simulation is necessarily more uncertain than the determination of T_A due to the extrapolations required.

There is another well-defined 'intermediate' characteristic temperature of glass formation which is useful in characterizing

glass-forming liquids and which can be determined accurately both experimentally and computationally. Over a restricted T range well above T_g and below T_A, τ can be well-described by an apparent power-law, $\tau \approx (T - T_c)^{-\gamma}$ where the fitted temperature T_c is conventionally termed the 'mode-coupling temperature' since such a power scaling is predicted by an idealized mean field mode-coupling theory of the dynamics of supercooled liquids. The power-law divergence of τ predicted by this theory does not actually occur in practice and the predicted T_c value does not correspond to the predictions of mode-coupling theory, but the approximate power scaling of τ seems to be general and T_c can thus be estimated in a reasonably well-defined fashion. In reality, T_c defines a 'crossover temperature' separating high and low T regimes of glass formation.[12] Equilibrium simulations of liquids are normally limited to $T > T_c$ because of the growing equilibration times of cooled liquids.

Acknowledgements

This work was partially supported by NIBIB Bioengineering Grant (# R01EB006398-0). Partial support from the UW MRSEC on Nanostructured Interfaces is also acknowledged.

References

1 A. Anopchenko, T. Psurek, D. VanderHart, J. F. Douglas and J. Obrzut, *Phys. Rev. E: Stat. Phys., Plasmas, Fluids, Relat. Interdiscip. Top.*, 2006, **74**, 031501.
2 T. Psurek, C. L. Soles, K. A. Page, M. T. Cicerone and J. F. Douglas, *J. Phys. Chem. B*, 2008, **112**, 15980.
3 R. A. Riggleman, J. F. Douglas and J. J. de Pablo, *J. Chem. Phys.*, 2007, **126**, 234903.
4 R. A. Riggleman, K. Yoshimoto, J. F. Douglas and J. J. de Pablo, *Phys. Rev. Lett.*, 2006, **97**, 045502.
5 R. A. Riggleman, J. F. Douglas and J. J. de Pablo, *Phys. Rev. E: Stat. Phys., Plasmas, Fluids, Relat. Interdiscip. Top.*, 2007, **76**, 011504.
6 S. Cukierman, J.-L. Halary and L. Monnerie, *J. Non-Cryst. Solids*, 1991, **131–133**, 898.
7 S. Cukierman, J.-L. Halary and L. Monnerie, *Polym. Eng. Sci.*, 1991, **31**, 1476.
8 T. Rouxel, *J. Am. Ceram. Soc.*, 2007, **90**, 3019.
9 F. Zok and F. F. Lange, *J. Am. Ceram. Soc.*, 1991, **74**, 1880.
10 J. Rodriguez, C. H. Allibert and J. M. Chaix, *Powder Technol.*, 1986, **47**, 25.
11 B. C. Mathur and P. K. Banerjee, *Br. Chem. Eng.*, 1967, **12**, 384.
12 J. Dudowicz, K. F. Freed and J. F. Douglas, *Adv. Chem. Phys.*, 2008, **137**, 125; E. Stukalin, J. F. Douglas and K. F. Freed, *J. Chem. Phys.*, 2009, **131**, 114905.
13 S. E. Abraham, S. M. Bhattacharrya and B. Bagchi, *Phys. Rev. Lett.*, 2008, **100**, 167801.
14 C. Donati, J. F. Douglas, W. Kob, S. J. Plimpton, P. H. Poole and S. C. Glotzer, *Phys. Rev. Lett.*, 1998, **80**, 2338; C. Donati, J. F. Douglas, W. Kob, S. J. Plimpton, P. H. Poole and S. C. Glotzer, 1997, arXiv:cond-mat/9706277v1.
15 J. F. Douglas, J. Dudowicz and K. Freed, *J. Chem. Phys.*, 2006, **125**, 144907. This work reviews numerous experimental and computational examples of dynamic heterogeneity.
16 C. Bennemann, C. Donati, J. Baschnagel and S. C. Glotzer, *Nature*, 1999, **399**, 246.
17 W. Kob, C. Donati, S. J. Plimpton, P. H. Poole and S. C. Glotzer, *Phys. Rev. Lett.*, 1997, **79**, 2827.
18 C. Donati, S. C. Glotzer, P. H. Poole, W. Kob and S. J. Plimpton, *Phys. Rev. E: Stat. Phys., Plasmas, Fluids, Relat. Interdiscip. Top.*, 1999, **60**, 3107.
19 A. H. Marcus, J. Schofield and S. A. Rice, *Phys. Rev. E: Stat. Phys., Plasmas, Fluids, Relat. Interdiscip. Top.*, 1999, **60**, 5725; B. Cui, B. Lin and S. A. Rice, *J. Chem. Phys.*, 2001, **114**, 9142.
20 E. R. Weeks, J. C. Crocker, A. C. Levitt, A. Schofield and D. A. Weitz, *Science*, 2000, **287**, 627.
21 C. A. Murray and R. A. Wenk, *Phys. Rev. Lett.*, 1989, **62**, 1643; C. A. Murray, D. H. Van Winkle and R. A. Wenk, *Phase Transitions*, 1990, **21**, 93; C. A. Murray and D. H. Van Winkle, *Phys. Rev. Lett.*, 1987, **58**, 1200.
22 R. J. Bathurst and L. Rothenburg, *Int. J. Eng. Sci.*, 1988, **26**, 373.
23 Y. Maeda and D. Paul, *J. Polym. Sci., Part B: Polym. Phys.*, 1987, **25**, 957.
24 R. Casalini, K. Ngai, C. Robertson and C. Roland, *J. Polym. Sci., Part B: Polym. Phys.*, 2000, **38**, 1841.
25 V. N. Novikov and A. P. Sokolov, *Nature*, 2004, **431**, 961.
26 S. N. Yannopoulos and G. P. Johari, *Nature*, 2006, **442**, E7; G. P. Johari, *Philos. Mag.*, 2006, **86**, 1567.
27 K. Yoshimoto, T. Jain, K. V. Workum, P. F. Nealey and J. J. De Pablo, *Phys. Rev. Lett.*, 2004, **93**, 175501.
28 F. W. Starr, S. Sastry, J. F. Douglas and S. C. Glotzer, *Phys. Rev. Lett.*, 2002, **89**, 125501.
29 G. Zaccai, *Science*, 2000, **288**, 1604.
30 A. Widmer-Cooper and P. Harrowell, *Phys. Rev. Lett.*, 2006, **96**, 185701.
31 A. P. Sokolov, R. Calemezuk, B. Salce, A. Kisliuk, D. Quitmann and E. Duval, *Phys. Rev. Lett.*, 1997, **78**, 2405.
32 F. Léonforte, A. Tanguy, J. P. Wittmer and J.-L. Barrat, *Phys. Rev. Lett.*, 2006, **97**, 055501.
33 F. Léonforte, R. Boissiere, A. Tanguy, J. P. Wittmer and J.-L. Barrat, *Phys. Rev. B: Condens. Matter*, 2005, **72**, 224206.
34 B. Rossi, G. Viliani, E. Duval, L. Angelani and W. Garber, *Europhys. Lett.*, 2005, **71**, 256.
35 W. Schirmacher, *Europhys. Lett.*, 2006, **73**, 892.
36 V. N. Novikov, Y. Ding and A. P. Sokolov, *Phys. Rev. E: Stat. Phys., Plasmas, Fluids, Relat. Interdiscip. Top.*, 2005, **71**, 061501.
37 C. Masciovecchio, G. Baldi, S. Caponi, L. Comez, S. Di Fonzo, D. Fioretto, A. Fontana, A. Gessini, S. C. Santucci, F. Sette, G. Viliani, P. Vilmercati and G. Ruocco, *Phys. Rev. Lett.*, 2006, **97**, 035501.
38 E. Maurer and W. Schirmacher, *J. Low Temp. Phys.*, 2004, **137**, 453.
39 J. S. Vrentas, J. L. Duda and H. C. Ling, *Macromolecules*, 1988, **21**, 1470.
40 B. J. Cauley, C. Cipriani, K. Ellis, A. K. Roy, A. A. Jones, P. T. Inglefield, B. J. McKinley and R. P. Kambour, *Macromolecules*, 1991, **24**, 403.
41 W. M. Lai, D. Rubin and E. Krempl, *Introduction to Continuum Mechanics*, Butterworth Heinemann, Burlington, MA, 1999.
42 D. A. McQuarrie, *Statistical Mechanics*, University Science Books, Sausalito, CA, 2000.
43 G. J. Papakonstantopoulos, R. A. Riggleman, J.-L. Barrat and J. J. De Pablo, *Phys. Rev. E: Stat. Phys., Plasmas, Fluids, Relat. Interdiscip. Top.*, 2008, **77**, 041502.
44 R. A. Riggleman and J. J. De Pablo, *J. Chem. Phys.*, 2008, **128**, 224504.
45 E. Bitzek, P. Koskinen, F. Gahler, M. Moseler and P. Gumbsch, *Phys. Rev. Lett.*, 2006, **97**, 170201.
46 M. Zhou, *Proc. R. Soc. London, Ser. A*, 2003, **459**, 2347.
47 M. L. Falk and J. S. Langer, *Phys. Rev. E: Stat. Phys., Plasmas, Fluids, Relat. Interdiscip. Top.*, 1998, **57**, 7192.
48 L. Larini, A. Ottochian, C. De Michele and D. Leporini, *Nat. Phys.*, 2008, **4**, 42.
49 E. W. Fischer, G. P. Hellman, H. W. Spiess, F. J. Hörth, U. Ecarius and M. Wehrle, *Makromol. Chem., Suppl.*, 1985, **12**, 189.
50 K. S. Schweizer and E. J. Saltzman, *J. Chem. Phys.*, 2003, **119**, 1181.
51 K. S. Schweizer and E. J. Saltzman, *J. Chem. Phys.*, 2004, **121**, 1984.
52 E. J. Saltzman and K. S. Schweizer, *J. Chem. Phys.*, 2004, **121**, 2001.
53 R. M. J. Cotterill, *Phys. Rev. Lett.*, 1979, **42**, 1541.
54 J. B. Bicerano and J. T. Seitz, in Molecular origin of toughening polymers, *Polymer Toughening*, ed. C. D. Arends, CRC Press, Marcel Dekker, 1996.
55 R. Zondervan, T. Xia, H. van der Meer, C. Storm, F. Kulzer, W. van Saarloos and M. Orrit, *Proc. Natl. Acad. Sci. U. S. A.*, 2008, **105**, 4993, See also: Zondervan and et al., *Proc. Natl. Acad. Sci. U. S. A.*, 2007, **104**, 12628.
56 S.-P. Chen, T. Egami and V. Vitek, *Phys. Rev. B: Condens. Matter*, 1988, **37**, 2440.
57 R. S. Lakes, *Nature*, 2001, **410**, 565.

58 R. S. Lakes, *Philos. Mag. Lett.*, 2001, **81**, 95; R. S. Lakes, *Phys. Rev. Lett.*, 2001, **86**, 2897.
59 Y. C. Wang and R. S. Lakes, *Am. J. Physiol.*, 2004, **42**, 40; Y. C. Wang and R. S. Lakes, *J. Appl. Phys.*, 2001, **90**, 6458.
60 V. N. Novikov, E. Rössler, V. K. Malinovsky and N. Surovtsev, *Europhys. Lett.*, 1996, **35**, 289.
61 T. S. Jain and J. J. de Pablo, *J. Chem. Phys.*, 2004, **120**, 9371.
62 W. Peng, H. E. Castillo, P. M. Goldbart and A. Zippelius, *Phys. Rev. B: Condens. Matter*, 1998, **57**, 839.
63 F. Starr and J. F. Douglas, *Phys. Rev. Lett.*, submitted.
64 A. Mermet, N. V. Surovtsev, E. Duval, J. F. Jal, J. Dupuy-Philon and A. J. Dianoux, *Europhys. Lett.*, 1996, **36**, 277.
65 T. Pang, *Phys. Rev. B: Condens. Matter*, 1992, **45**, 2490.
66 H. E. Stanley, *Introduction to Phase Transitions and CriticalPhenomena*, Oxford University Press, New York, 1971.
67 E. W. Fischer, Ch. Becker, J.-U. Hagenah and G. Meier, *Prog. Colloid Interface Sci.*, 1989, **80**, 198.
68 A. Patkowski, Th. Thurn-Albrecht, E. Banachowicz, W. Steffen, P. Bösecke, T. Narayanan and E. W. Fischer, *Phys. Rev. E: Stat. Phys., Plasmas, Fluids, Relat. Interdiscip. Top.*, 2000, **61**, 6909.
69 A. Patkowski, E. W. Fischer, W. Steffen, H. Gläser, M. Baumann, T. Ruths and G. Meier, *Phys. Rev. E: Stat. Phys., Plasmas, Fluids, Relat. Interdiscip. Top.*, 2001, **63**, 061503.
70 Z. Hu and C. J. Margulis, *Proc. Natl. Acad. Sci. U. S. A.*, 2008, **103**, 4993.
71 D. J. Bicout and G. Zaccai, *Biophys. J.*, 2001, **80**, 1115.
72 T. E. Dirama, G. A. Carri and A. P. Sokolov, *J. Chem. Phys.*, 2005, **122**, 114505.
73 K. Yoshimoto, T. S. Jain, P. F. Nealey and J. J. de Pablo, *J. Chem. Phys.*, 2005, **122**, 144712.
74 H.-N. Lee, R. A. Riggleman, J. J. de Pablo and M. D. Ediger, *Macromolecules*, 2009, **42**, 4328.
75 F. M. Capaldi, M. C. Boyce and G. C. Rutledge, *Phys. Rev. Lett.*, 2002, **89**, 175505.
76 C. J. Ellison, R. L. Ruszkowski, N. J. Fredin and J. M. Torkelson, *Phys. Rev. Lett.*, 2004, **92**, 095702.
77 S. E. B. Petrie, R. S. Moore and J. R. Flick, *J. Appl. Phys.*, 1972, **43**, 4318.
78 C. C. Seow, P. B. Cheah and Y. P. Chang, *J. Food Sci.*, 1999, **64**, 576.
79 M. Peleg, *Cereal Chem.*, 1996, **73**, 712.
80 M. Peleg, *Rheol. Acta*, 1993, **35**, 575.
81 P. Zhang and R. L. Whistler, *J. Appl. Polym. Sci.*, 2004, **93**, 2896.
82 Y. Zheng and G. B. McKenna, *Macromolecules*, 2003, **36**, 2387.
83 K. Ninjo and T. Nakagawa, *Polym. J. (Tokyo)*, 1973, **4**, 143.
84 B. J. Berger, C. C. Haberger and B. M. Pankonin, The influence of temperature and moisture on the ultrasonic viscoelastic properties of cellulose, *IPC Technical Paper Series*, The Institute of Paper Chemistry, Appleton, Wisconsin, 1988, 283.
85 G. P. Johari and M. Goldstein, *J. Chem. Phys.*, 1970, **53**, 2372.
86 S. P. Delcambre, R. A. Riggleman, J. J. de Pablo and P. F. Nealey, *Soft Matter*, in preparation.
87 T. R. Bohme and J. J. de Pablo, *J. Chem. Phys.*, 2002, **116**, 9939.
88 K. Yoshimoto, M. P. Stoykovich, H. B. Cao, J. J. de Pablo, P. F. Nealey and W. J. Drugan, *J. Chem. Phys.*, 2004, **96**, 1857.
89 R. E. Cais, M. Nozomi, M. Kawai and A. Miyake, *Macromolecules*, 1992, **25**, 4588.
90 R. Zondervan, T. Xia, H. van der Meer, C. Storm, F. Kulzer, W. van Saarloos and M. Orrit, *Proc. Natl. Acad. Sci. U. S. A.*, 2008, **105**, 4993.
91 R. Zondervan, F. Kulzer, G. C. G. Berkhout and M. Orrit, *Proc. Natl. Acad. Sci. U. S. A.*, 2007, **104**, 12628.
92 Z. H. Hu and C. J. Margulis, *Proc. Natl. Acad. Sci. U. S. A.*, 2006, **103**, 831.
93 M. Dzugutov, S. I. Simdyankin and F. H. M. Zetterling, *Phys. Rev. Lett.*, 2002, **89**, 195701.
94 F. H. M. Zetterling, M. Dzugutov and S. I. Simdyankin, *J. Non-Cryst. Solids*, 2001, **293–295**, 39.
95 A. V. Anikeenko and N. N. Medvedev, *Phys. Rev. Lett.*, 2007, **98**, 235504.
96 A. V. Anikeenko, N. N. Medvedev and T. Aste, *Phys. Rev. E: Stat. Phys., Plasmas, Fluids, Relat. Interdiscip. Top.*, 2008, **77**, 031101.
97 C. Donati, S. C. Glotzer, P. H. Poole, W. Kob and S. J. Plimpton, *Phys. Rev. E: Stat. Phys., Plasmas, Fluids, Relat. Interdiscip. Top.*, 1997, **60**, 3107.
98 G. Parisi and N. Sourlas, *Phys. Rev. Lett.*, 1981, **46**, 871.
99 M. L. Wallace, B. Joos and M. Plischke, *Phys. Rev. E: Stat. Phys., Plasmas, Fluids, Relat. Interdiscip. Top.*, 2004, **70**, 041501.
100 L. Golubović and T. C. Lubenski, *Phys. Rev. Lett.*, 1989, **63**, 1082.
101 H. A. Makse, N. Gland, D. L. Johnson and L. Schwartz, *Phys. Rev. E: Stat. Phys., Plasmas, Fluids, Relat. Interdiscip. Top.*, 2004, **70**, 061302.
102 K. W. Wojciechowski, K. V. Tretiakov and M. Kowalik, *Phys. Rev. E: Stat. Phys., Plasmas, Fluids, Relat. Interdiscip. Top.*, 2003, **67**, 036121.
103 V. V. Novikov, K. W. Wojciechowski, D. V. Belov and V. P. Privalko, *Phys. Rev. E: Stat. Phys., Plasmas, Fluids, Relat. Interdiscip. Top.*, 2001, **63**, 036120.
104 B. Brandel and R. S. Lakes, *J. Mater. Sci.*, 2001, **36**, 5885.
105 G. Wei, *J. Chem. Phys.*, 1992, **96**, 3226.
106 A. Tanguy, F. Leonforte, J. P. Wittmer and J. L. Barrat, *Appl. Surf. Sci.*, 2004, **22**, 282.

